1993PASP..105..940M

Publications of the Astronomical Society of the Pacific
**105:** 940–944, 1993 September

# Observations of the OH Airglow Emission

TOSHINORI MAIHARA AND FUMIHIDE IWAMURO

Department of Physics, Kyoto University, Kitashirakawa, Kyoto 606, Japan
Electronic mail: maihara@cr.scphys.kyoto-u.ac.jp, iwamuro@cr.scphys.kyoto-u.ac.jp

TAKUYA YAMASHITA

National Astronomical Observatory of Japan, Mitaka, Tokyo 181, Japan
Electronic mail: oyamash@cl.mtk.nao.ac.jp

DONALD N. B. HALL, LENNOX L. COWIE, ALAN T. TOKUNAGA, AND ANDREW PICKLES

Institute for Astronomy, University of Hawaii, 2680 Woodlawn Drive, Honolulu, Hawaii 96822
Electronic mail: hall@hubble.ifa.hawaii.edu, cowie@hubble.ifa.hawaii.edu, tokunaga@galileo.ifa.hawaii.edu, pickles@galileo.ifa.hawaii.edu

*Received 1992 October 29; accepted 1993 June 17*

**ABSTRACT.** The OH airglow emission in the $J$ and $H$ bands was observed for the purpose of determining the linewidths, the precise wavelengths of individual lines, and also the continuum emission level between lines. The lines were not resolved with a resolving power of about 17,000. Wavelengths and intensities were measured for approximately 120 lines from 1.1 to 1.8 $\mu$m. The continuum emission intensity was also measured on a dark night and was as low as 590 photons $s^{-1}$ $m^{-2}$ $arcsec^{-2}$ $\mu m^{-1}$ at 1.665 $\mu$m. The level is about one-fiftieth the average flux of the OH airglow emission in the $H$ band.

## 1. INTRODUCTION

The OH airglow emission consists of a number of strong emission lines and is the dominant background radiation source in the near-infrared region, especially from 1 to 2 $\mu$m. The OH airglow severely restricts astronomical observations of faint objects in these spectral bands. It has therefore been desired to make ground-based observations with special preoptics capable of filtering out the OH lines. The present observations of the OH airglow emission were made in order to determine the wavelengths of each line precisely enough to design the OH suppressing preoptics system, and also to measure the continuum emission level between the lines. With the information obtained, we have successfully designed and built such a preoptics system for low-resolution spectroscopy which will be described elsewhere (Maihara et al. 1993).

## 2. OBSERVATIONS

The observations were made with the coudé spectrometer of the University of Hawaii 2.2-m telescope atop Mauna Kea, Hawaii. The focal plane detector of the spectrometer is the 256×256 HgCdTe (NICMOS 3) array currently being used as a near-infrared camera at the Cassegrain focus (Hodapp et al. 1992). The observing log used in the series of observations is summarized in Table 1.

The integration time for a single exposure on the OH airglow was set at 250 s throughout the observations, except for special frames intended to provide flats and calibrations. Frames for flatfielding with various exposure times were utilized to identify and record bad pixels by testing their linearity, and this was used to create a mask of bad pixels to be removed. When the continuum emission was measured, we took 20 frames to reduce statistical errors for the faint continuum emission. The detailed procedure of measurement will be described in the following section.

For wavelength calibration, an argon discharge lamp was inserted in front of the coudé slit to record Ar reference lines in the frames at the respective grating settings. The central wavelength of each OH line was derived by reference to at least two recorded Ar lines. For flux calibration we observed two standard stars (HD 162208 and HD 193514) in the second observing run, by which we have estimated the overall throughput of this spectroscopic measurement of about 2.5% including the detector's quantum efficiency. All observations were made mostly around the local midnight.

## 3. RESULTS

In the first observing run, we obtained spectral features of typical OH emission lines in the $H$ band. This is shown in Fig. 1, where we compare them to the previous observations made by Moorwood (1987) with medium-resolution spectroscopy. The actual resolving power attained in the present observation was roughly 17,000, and the profile does not exhibit any intrinsic breadth when compared with the Ar calibration lines. Obviously individual lines are quite narrow without any wing broadening as expected and the region between lines is clear without any detectable emission.

In the second observing run, we measured all the detectable lines from 1.1 to 1.8 $\mu$m. The number of lines measured in the $J$ band is 53, including a couple of $O_2$ lines, and is 69 in the $H$ band. The result as listed by the vacuum wavelength is presented together with the measurements by Steed and Baker (1979) in Tables 2(a) and 2(b) for the $J$ and $H$ band, respectively. The wavelength of



© 1993. Astronomical Society of the Pacific

© Astronomical Society of the Pacific • Provided by the NASA Astrophysics Data System

1993PASP..105..940M



TABLE 1
The Observing Log

| Items | January 1991 | July 1991 | February 1992 |
|---|---|---|---|
| Slit | 0.3x50mm²(0.″83x2.′3) | 2x50mm²(5.″5x2.′3) | 2.3x50mm²(6.″3x2.′3) |
| Grating | 600 gr/mm, 1.32μm[1] | 400 gr/mm, 1.20μm[1] | 400 gr/mm, 1.20μm[1] |
| Dispersion | 0.65 Å/pixel | 0.97Å/pixel | 0.49Å/pixel |
| Resolving Power[4] | 16500 | 2200 | 1900 |

1) Blaze wavelength.
2) Instruments used are the Coude spectrometer in conjunction with the NICMOS camera (256x256 HgCdTe) attached to the University of Hawaii 2.2m telescope.
3) The focal length of the collimator is 6.7m, and that of the camera mirror is 1.22m.
4) Measured spectral resolving power.

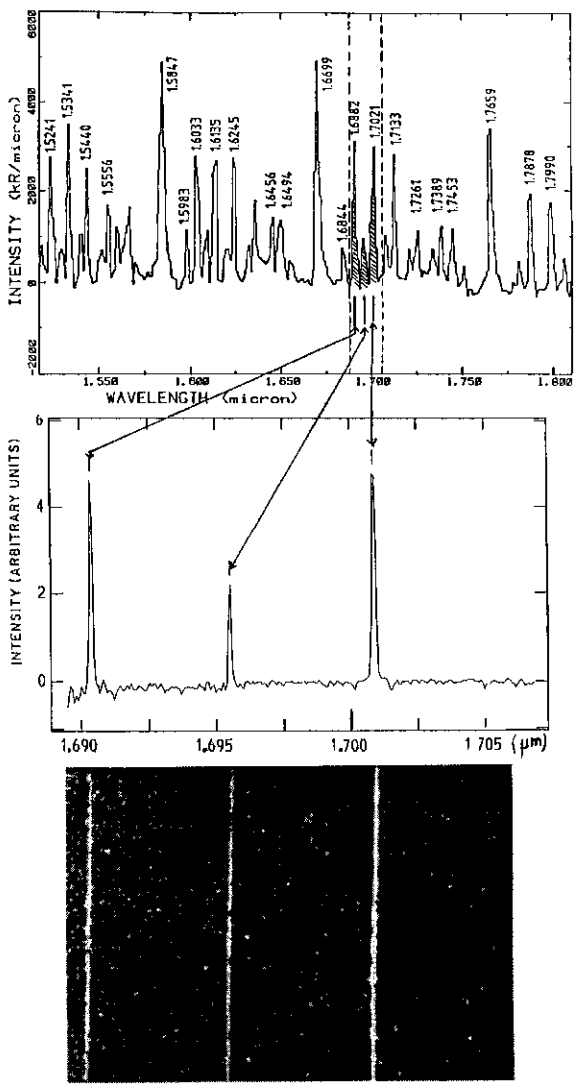


FIG. 1—An example of observed OH line profiles at around 1.7 μm. The upper panel is reproduced from Moorwood (1987) for comparison, the middle panel is the line profile obtained, and the lowest panel is the spectral image of the present measurement.

each line was determined by Ar lamp lines measured just before or after taking OH line frames. Since the wavelength span of a single exposure was typically as narrow as 250 Å, for example, in the *H* band, the nonlinearity between pixel number and wavelength could be neglected. In fact, the linearity check with several Ar lines recorded in a calibration frame has proved that the deviation is smaller than 0.2 Å. Another source of error in the wavelength determination arises from distorted line profiles of weak lines due to low SN ratio caused by unstable and/or noisy pixels of the NICMOS array detector. As a result, with these error sources, we have estimated uncertainties in wavelength of typically ±0.5 Å, except for several weakest lines of about ±1 Å; one should take this into account when Table 2 is referred to.

One may notice there are discrepancies for a few number of lines between our measurement and the measurement of Steed and Baker. These are partly ascribable to the sensitivity limit of our measurement at the faintest ends. In the short-wavelength edge of *H* band, i.e., shorter than 1.52 μm, we have missed a couple of lines due to the falling transmission of the *H*-band filter. Meanwhile the lines around 1.27 μm in our measurement are $O_2$ lines which are

TABLE 2a
Detected Lines in the *J* Band

| Number | Wavelength λ μm(in vacuum) | Intensity γ s⁻¹m⁻²arcsec⁻² | λ (Steed & Baker) μm(in vacuum) | Intensity kR |
|---|---|---|---|---|
| 1 | 1.14398 | 22 | 1.14364 | 0.40 |
| 2 | 1.14516 | 17 | | |
| 3 | 1.15390 | 45 | 1.15395 | 0.32 |
| 4 | 1.15912 | 54 | 1.15925 | 0.35 |
| | | | 1.16285 | 0.12 |
| 5 | 1.16517 | 38 | 1.16515 | 0.30 |
| | | | 1.16965 | 0.08 |
| 6 | 1.17164 | 92 | 1.17165 | 0.20 |
| | | | 1.17875 | 0.08 |
| 7 | 1.19744 | 25 | | |
| 8 | 1.19880 | 30 | | |
| 9 | 1.20009 | 11 | 1.20016 | 0.12 |
| 10 | 1.20068 | 44 | 1.20076 | 0.20 |
| 11 | 1.20241 | 25 | 1.20256 | 0.18 |
| 12 | 1.20313 | 85 | 1.20316 | 0.24 |
| 13 | 1.20564 | 26 | 1.20559 | 0.07 |
| 14 | 1.21234 | 111 | 1.21226 | 0.54 |
| 15 | 1.21384 | 40 | 1.21359 | 0.20 |
| 16 | 1.21560 | 18 | 1.21550 | 0.05 |
| 17 | 1.21968 | 38 | 1.21964 | 0.11 |
| 18 | 1.22290 | 109 | 1.22293 | 0.40 |
| 19 | 1.22579 | 59 | 1.22578 | 0.18 |
| 20 | 1.22872 | 113 | 1.22870 | 0.46 |
| 21 | 1.23259 | 22 | 1.23259 | 0.17 |
| 22 | 1.23508 | 82 | 1.23516 | 0.30 |
| | | | 1.24009 | 0.11 |
| 23 | 1.24235 | 114 | 1.24230 | 0.19 |
| 24 | 1.25038 | 31 | 1.25024 | 0.09 |
| | | | 1.25891 | 0.05 |
| 25 | 1.26857 | 80 | | |
| 26 | 1.26951 | 64 | | |
| 27 | 1.27020 | 37 | | |
| 28 | 1.27104 | 39 | | |
| 29 | 1.27261 | 20 | | |
| 30 | 1.27446 | 24 | | |
| 31 | 1.27529 | 45 | 1.27528 | 0.15 |
| 32 | 1.27636 | 76 | 1.27644 | 0.21 |
| 33 | 1.27760 | 32 | | |
| 34 | 1.27831 | 149 | 1.27825 | 0.24 |
| 35 | 1.27980 | 57 | | |
| 36 | 1.28065 | 107 | 1.28070 | 0.23 |
| 37 | 1.28248 | 25 | | |
| 38 | 1.28346 | 58 | 1.28346 | 0.08 |
| 39 | 1.28450 | 35 | | |
| 40 | 1.28660 | 31 | | |
| 41 | 1.29054 | 261 | 1.29057 | 0.57 |
| 42 | 1.29213 | 84 | 1.29212 | 0.17 |
| 43 | 1.29434 | 26 | 1.29431 | 0.09 |
| 44 | 1.29861 | 67 | 1.29857 | 0.15 |
| 45 | 1.30218 | 187 | 1.30216 | 0.32 |
| 46 | 1.30530 | 82 | 1.30528 | 0.21 |
| 47 | 1.30861 | 277 | 1.30852 | 0.39 |
| 48 | 1.31285 | 99 | 1.31278 | 0.18 |
| 49 | 1.31577 | 77 | 1.31567 | 0.19 |
| 50 | 1.32115 | 47 | 1.32110 | 0.10 |
| 51 | 1.32368 | 104 | 1.32366 | 0.27 |
| 52 | 1.33244 | 29 | 1.33247 | 0.04 |
| 53 | 1.34220 | 26 | 1.34208 | 0.06 |

© Astronomical Society of the Pacific • Provided by the NASA Astrophysics Data System

1993PASP..105..940M



TABLE 2b
Detected Lines in the *H* Band

| Number | Wavelength λ μm(in vacuum) | Intensity γ s$^{-1}$m$^{-2}$arcsec$^{-2}$ | λ (Steed & Baker) μm(in vacuum) | Intensity kR |
|---|---|---|---|---|
| 1 | 1.50564 | 102 | 1.50555 | 1.95 |
| 2 | 1.50692 | 8 | 1.50689 | 0.66 |
| | | | 1.50882 | 0.23 |
| | | | 1.51137 | 0.10 |
| 3 | 1.51877 | 20 | 1.51870 | 0.38 |
| 4 | 1.52410 | 90 | 1.52410 | 1.41 |
| 5 | 1.52879 | 45 | 1.52878 | 0.58 |
| 6 | 1.53329 | 177 | 1.53324 | 1.15 |
| 7 | 1.53954 | 54 | 1.53953 | 0.40 |
| 8 | 1.54323 | 163 | 1.54321 | 1.08 |
| | | | 1.54621 | 0.10 |
| 9 | 1.55013 | 17 | 1.55008 | 0.20 |
| 10 | 1.55101 | 44 | 1.55098 | 0.25 |
| 11 | 1.55176 | 20 | 1.55179 | 0.20 |
| 12 | 1.55406 | 71 | 1.55404 | 0.55 |
| 13 | 1.55465 | 44 | 1.55462 | |
| 14 | 1.55701 | 32 | 1.55702 | 0.15 |
| 15 | 1.55976 | 113 | 1.55977 | 0.70 |
| 16 | 1.56316 | 56 | 1.56316 | 0.35 |
| 17 | 1.56555 | 188 | 1.56550 | 1.05 |
| 18 | 1.57026 | 41 | 1.57025 | 0.28 |
| 19 | 1.57597 | 8 | 1.57603 | 0.10 |
| | | | 1.57821 | 0.15 |
| 20 | 1.58334 | 338 | 1.58332 | 2.30 |
| 21 | 1.58484 | 92 | 1.58481 | 0.90 |
| 22 | 1.58689 | 29 | 1.58693 | 0.25 |
| | | | 1.58973 | 0.10 |
| 23 | 1.59725 | 100 | 1.59726 | 0.50 |
| 24 | 1.60312 | 299 | 1.60308 | 1.53 |
| 25 | 1.60804 | 125 | 1.60798 | 0.65 |
| 26 | 1.61290 | 296 | 1.61286 | 1.71 |
| 27 | 1.61949 | 61 | 1.61947 | 0.63 |
| 28 | 1.62351 | 297 | 1.62354 | 1.27 |
| 29 | 1.63051 | 19 | | |
| 30 | 1.63175 | 72 | 1.63172 | 0.27 |
| 31 | 1.63421 | 56 | 1.63418 | 0.12 |
| 32 | 1.63520 | 138 | 1.63513 | 0.65 |
| 33 | 1.63606 | 24 | 1.63604 | 0.10 |
| 34 | 1.63888 | 51 | 1.63885 | 0.25 |
| 35 | 1.64149 | 16 | 1.64147 | 0.20 |
| 36 | 1.64421 | 174 | 1.64421 | |
| 37 | 1.64478 | 19 | 1.64476 | 0.70 |
| 38 | 1.64783 | 83 | 1.64790 | 0.50 |
| 39 | 1.65027 | 152 | 1.65023 | 0.75 |
| 40 | 1.65541 | 92 | 1.65539 | 0.30 |
| 41 | 1.66111 | 20 | 1.66110 | 0.10 |
| 42 | 1.66925 | 431 | 1.66921 | 2.30 |
| 43 | 1.67091 | 144 | 1.67088 | 0.83 |
| 44 | 1.67328 | 46 | 1.67325 | 0.30 |
| | | | 1.67636 | 0.15 |
| 45 | 1.68404 | 71 | 1.68405 | 0.30 |
| 46 | 1.69034 | 244 | 1.69037 | 1.45 |
| 47 | 1.69552 | 122 | 1.69551 | 0.52 |
| 48 | 1.70083 | 301 | 1.70088 | 1.80 |
| 49 | 1.70783 | 82 | 1.70783 | 0.70 |
| 50 | 1.71235 | 199 | 1.71236 | 1.20 |
| 51 | 1.72105 | 60 | 1.72104 | 0.36 |
| 52 | 1.72484 | 107 | 1.72486 | 0.70 |
| 53 | 1.72826 | 47 | 1.72829 | 0.18 |
| 54 | 1.73032 | 12 | | |
| 55 | 1.73311 | 58 | 1.73309 | 0.32 |
| 56 | 1.73519 | 53 | 1.73511 | 0.20 |
| 57 | 1.73601 | 42 | 1.73597 | 0.20 |
| | | | 1.73838 | 0.40 |
| 58 | 1.73865 | 186 | 1.73867 | 0.40 |
| 59 | 1.74275 | 45 | 1.74270 | 0.30 |
| 60 | 1.74499 | 160 | 1.74499 | 0.72 |
| 61 | 1.75010 | 9 | 1.75013 | 0.27 |
| 62 | 1.75063 | 55 | 1.75060 | 0.08 |
| 63 | 1.75294 | 28 | 1.75294 | 0.08 |
| 64 | 1.76531 | 363 | 1.76532 | 2.00 |
| 65 | 1.76721 | 130 | 1.76718 | 0.70 |
| 66 | 1.76987 | 52 | 1.76984 | 0.18 |
| 67 | 1.78115 | 72 | 1.78114 | 0.08 |
| 68 | 1.78808 | 268 | 1.78803 | 1.20 |
| | | | 1.79348 | 0.05 |
| 69 | 1.79942 | 204 | 1.79940 | 1.42 |

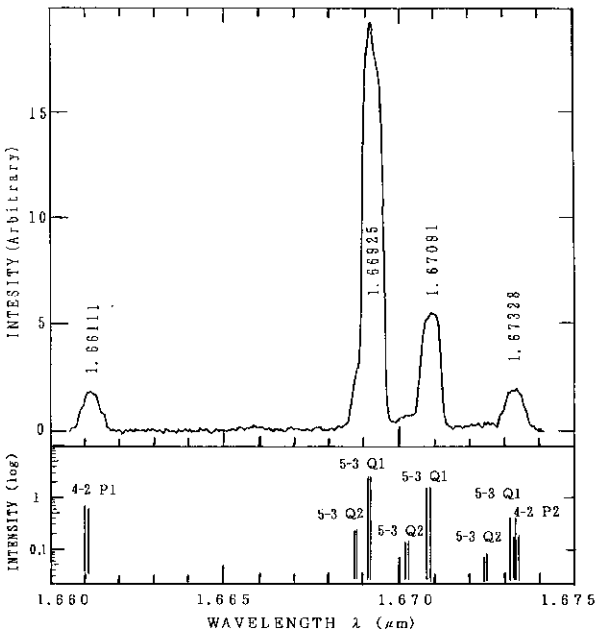


FIG. 2—The coadded spectrum of the measured OH emission between 1.661 and 1.674 μm (upper panel), compared with the high-resolution data of the laboratory OH emission (lower panel) taken by Hubbard and Brault (1993) with the FTS.

not listed in Steed and Baker. Some $N_2$ lines at about 1.19 μm are also detected and listed only in our table.

In the third observing run on a dark night, the continuum level of the sky emission between OH lines was measured. The continuum emission has been derived from pairs of frames: the first one was an exposure with the upper portion of the slit being closed, and the second one was that with the lower portion of the slit being closed. The unexposed portion was subtracted from the exposed portion in the two pairing frames to get two half frames. Then the continuum intensity count is obtained by averaging the two half frames. The whole observation consists of 20 frames or ten pairs in all. By this measurement technique, we are able to deduce the apparent intensity from the average count in the area of 120 pixels (60 Å) × 100 pixels (70 arcsec) between two OH lines at 1.66111 and 1.66925 μm. This procedure has been proved to be quite effective in deriving the average emission by minimizing the effect of nonuniformity of the detector, the dark current, and its temporal drift. The obtained sky brightness of the emission between lines at 1.665 μm which we presumed to be continuum emission is $590 \pm 140$ photons s$^{-1}$ m$^{-2}$ arcsec$^{-2}$ μm$^{-1}$ at one air mass. The photometric calibration was based on the measurement of a 7.13 *H*-mag reference star: HD 136754 (Elias et al. 1982), deriving a total throughput of the spectrograph including atmospheric transmission, telescope, and detector quantum efficiency of 2.4%, almost the same as that measured in the second observing run. Displayed in Fig. 2 is a coadded spectrum using the frames of the above differential measurements, compared with the laboratory data of OH lines taken by the FTS (Hubbard and Brault 1993). Apparently there is no line in the spectral range where we measured continuum, implying that the detected emission is of continuum, not of faint line emissions.

It should be noted that the result was quite different on a bright night, when we measured the continuum emission level in the second observing run by exactly the same method. The brightness obtained in the same wavelength region was as high as 9100 photons s$^{-1}$ m$^{-2}$ arcsec$^{-2}$ μm$^{-1}$ in the direction close to the near full moon. It has been found as described in the following section that the observed brightness can be explained by the scattered moon light by the stratospheric dust layer produced in the volcanic eruption of Mt. Pinatubo in the Philippines.

© Astronomical Society of the Pacific • Provided by the NASA Astrophysics Data System

1993PASP..105..940M



## 4. DISCUSSION

### 4.1 Line Emission

The OH airglow consists of numerous emission lines in the near-infrared which are both spatially and temporally variable, and it is a serious problem for astronomical observations of faintest objects. The line intensities of the individual lines were measured by Steed and Baker (1979). The number of lines they tabulated in their report is 52 in our $J$ passband, i.e., 1.12 to 1.34 $\mu$m, while we have detected and given intensities of 53 lines including $O_2$ lines near 1.27 $\mu$m. On the other hand, we have measured 69 lines in our $H$ passband, compared with 73 lines given by Steed and Baker (1979). A few discrepancies between the data could be attributed in part to the insufficient detectivity of our measurements. The total integrated line intensity we obtained in the $J$ band is 3700 photons $s^{-1}\,m^{-2}\,arcsec^{-2}\,band^{-1}$ or 17000 photons $s^{-1}\,m^{-2}\,arcsec^{-2}\mu m^{-1}$. Similarly, the integrated intensity in the $H$ band is 7400 photons $s^{-1}\,m^{-2}\,arcsec^{-2}\,band^{-1}$, or 26,000 photons $s^{-1}\,m^{-2}\,arcsec^{-2}\,\mu m^{-1}$. Both intensities are roughly consistent with measurements reported so far, although the measurement by Ramsay et al. (1992) seems to give appreciably higher line intensities.

The applicability of the atmospheric OH lines in the visible and near-infrared regions ($\leqslant 1.1$ $\mu$m) as wavelength standard for astronomical spectroscopy has been examined by Osterbrock and Martel (1992). Table 2 obtained in the present observations can also be utilized as the wavelength standard in spectroscopic observations with low to medium resolutions. As described in the previous section, the typical wavelength uncertainty of the lines in Table 2 is $\pm 0.5$ Å, and for weakest lines, $\pm 1$ Å. Taking these errors into account, the tabulated OH and other molecular lines should be utilized with care. For instance, $Q$ branches are made of a series of lines within a few tens of angstroms, and they look like asymmetric broad lines with a low-resolution measurement as appeared in the upper panel of Fig. 1, which refers to the observation with a resolving power of about 600 by Moorwood (1987).

In our observation with the highest resolving power, we measured a line-width of approximately 1 Å for the lines presented in Fig. 1, just being the instrumental width. The actual OH lines are basically fine-structure doublets, and they are sometimes made of triplets or quadruples. For example, the 1.69034 line in Fig. 1 is made of three 5-3 P1 lines within a 0.45 Å range. Note that the intrinsic width of each line must be of the order of 0.1 Å, since the kinetic temperature is around 220 K (see, e.g., Baker et al. 1973) and the pressure broadening is negligible at this density.

### 4.2 Continuum

The continuum intensity between OH lines in the near-infrared has been measured for the first time by the present observations. The intensity level we have measured, 590 photons $s^{-1}\,m^{-2}\,arcsec^{-2}\,\mu m^{-1}$ at $\lambda \sim 1.665$ $\mu$m, is a little higher than 280 photons $s^{-1}\,m^{-2}\,arcsec^{-2}\,\mu m^{-1}$ estimated by McCaughrean (1988). He used the measured continuum at 0.85 $\mu$m by Noxon (1978) of 130 photons $s^{-1}\,m^{-2}\,arcsec^{-2}\,\mu m^{-1}$ and extrapolated it to the near-infrared. Wraight (1977) tried to interpret the continuum emission in the nightglow with the radiative association reaction: $O+NO \rightarrow NO_2+\gamma$. He presented a calculated radiance of about 7 $R$/Å, or 1300 photons $s^{-1}\,m^{-2}\,arcsec^{-2}\,\mu m^{-1}$ at 1 $\mu$m, whose spectrum appeared to rise slightly toward longer wavelengths. Although there seem to be ambiguous factors in physical conditions of the atmosphere he adopted, this emission mechanism may be a possible candidate to explain the detected continuum.

Other possible sources of continuum are predicted to be weaker. The zodiacal light is estimated to have a brightness an order of magnitude fainter than the measured one toward the direction we observed (elongation $\epsilon \sim 140°$, and ecliptic latitude $b \sim 40°$). Galactic and extragalactic diffuse light is even fainter except in the direction toward the galactic plane. The atmospheric scattered light due to scattering of the galactic light by aerosol particles also does not make a significant contribution to the measured continuum. It is hard to assess the contribution of a light source in the dome room, but it is not very likely that the residual dome light, if any, affects the measurement considerably, because the beam from the telescope mirror system to the coudé exit near the slit is enclosed.

As described in the previous section, the continuum emission level measured on the night of 1991 July 25 was much higher than the intensity presented above. This is probably attributed to the scattered moonlight by the Pinatubo-associated ash/aerozol particles in the lower stratosphere. The observed line of sight was fairly close to the direction ($\sim 20°$) to the near full moon. In fact, the $V$-band extinctions of 0.25–0.4 mag/airmass due to the Pinatubo dust clouds were reported by Mauna Kea observatories in the period of late July 1991. This implies a column density of about $10^7$ particles $cm^{-2}$ assuming a radius of dust as 1 $\mu$m. The surface brightness of the scattered light depends on the angular distance from the moon which is related to the phase function of scattering. It is shown that with the simple calculation based on the Mie scattering theory, the intensity level of the scattered light of the moon (assuming $H \sim -13$ mag during the observation) is in the range of a few $10^3$–$10^4$ photons $s^{-1}\,m^{-2}\,arcsec^{-2}\,\mu m^{-1}$ in the $H$ band depending on the parameters such as size and refractive index. Therefore, it is very likely that the observed continuum intensity in the bright night could be attributed to the moonlight scattered by the fairly thick aerozol layer.

### 4.3 Astronomical Implication

The present spectroscopic measurements of the whole range of both $J$ and $H$ bands of OH emission lines have provided necessary information to design and build an OH airglow suppressing spectrograph. The measured continuum intensity of about 600 photons $s^{-1}\,m^{-2}\,arcsec^{-2}\,\mu m^{-1}$ at about 1.67 $\mu$m is still quite low compared to the average flux of about 30,000 photons $s^{-1}\,m^{-2}\,arcsec^{-2}\,\mu m^{-1}$ in the $H$ band.

Based on the results presented here, it is concluded that

© Astronomical Society of the Pacific • Provided by the NASA Astrophysics Data System

1993PASP..105..940M



if we could perfectly eliminate OH emission lines by a specially designed spectroscopic filter, the background flux onto a detector will be reduced to about 2% of the usual level. In a prototype instrument developed by us, we cannot eliminate all OH lines, especially very weak ones, resulting in a background reduction of 3% or so. The expected gain in terms of limiting magnitude is roughly 1.5–2 mag. The benefit of removing OH lines would be not only the reduction of background, but also the longer integration time that will be possible without being affected by the annoying spatial and temporal variation of the OH airglow emission.

## REFERENCES

Baker, D. J., Steed, A. J., and Stair, Jr., A. T. 1973, J. Geophys. Res., 78, 8859
Elias, J. H., Frogel, J. A., Matthews, K., and Neugebauer, G. 1982, AJ, 87, 1029
Hodapp, K-W., Rayner, J., and Irwin, E. 1992, PASP, 104, 441
Hubbard, R., and Brault, J. 1993, private communication
Maihara, T., Iwamuro, F., Yamashita, T., Hall, D. N. B., Cowie, L. L., Tokunaga, A. T., and Pickles, A. 1993, SPIE No. 1946, in press
McCaughrean, M. J. 1988, Ph.D. thesis, University of Edinburgh
Moorwood, A. F. W. 1987, in Infrared Astronomy with Arrays, ed. C. G. Wynn-Williams and E. E. Becklin (Honolulu, University of Hawaii), p. 379
Noxon, J. F. 1978, Planet. Space Sci., 26, 191
Osterbrock. D. E., and Martel, A. 1992, PASP, 104, 76
Outred, M. 1978, J. Phys. Chem. Ref. Data 7, 1
Ramsay, S. K., Mountain, C. M., and Geballe, T. R. 1992, MNRAS, 259, 751
Steed, A. J., and Baker, D. J. 1979, Appl. Opt., 18, 3386
Wraight, P. C. 1977, Planet. Space Sci., 25, 787

© Astronomical Society of the Pacific • Provided by the NASA Astrophysics Data System

1993PASP..105..940M

Publications of the Astronomical Society of the Pacific
**105:** 945–945, 1993 September

# The Second Hubble Fellows Symposium

COLIN A. NORMAN

Space Telescope Science Institute, 3700 San Martin Drive, Baltimore, Maryland 21218
Electronic mail: norman@stsci.edu

The Hubble Fellowship Program is administered by the Space Telescope Science Institute with funding from the National Aeronautics and Space Administration. Beginning in September 1990, the program has awarded fellowships to outstanding recent Ph.D.s in astronomy and astrophysics. This support allows the Hubble Fellows to conduct postdoctoral research at U.S. institutions in areas of study broadly related to the mission of the *Hubble Space Telescope.*

The second annual Hubble Fellows Symposium was held at the Space Telescope Science Institute on November 9, 10, and 11, 1992. Each of the Hubble Fellows gave a presentation of his or her latest research work. Twenty-six papers were submitted. Hubble Fellows who were not able to attend were invited to submit papers. The breadth of the Hubble Fellowship program is illustrated by topics ranging from studies of our own galaxy to the most distant quasars.

Special thanks are due to: Marjorie Shettle, Barbara Jedrzejewski, Lisa Spurrier, and Tawanta Nance who helped organize the Symposium; to Ray Beaser and Elyse Wagner for their administrative support; to Ray Villard for the public-affairs interface; and to Howard Bond and Denise Dankert who have assisted in the publication of the proceedings in this issue of the *Publications.* The Space Telescope Science Institute is operated by the Association of Universities for Research in Astronomy, Inc., for the National Aeronautics and Space Administration under NASA Contract No. NAS 5-26555.



© 1993. Astronomical Society of the Pacific

© Astronomical Society of the Pacific • Provided by the NASA Astrophysics Data System